

HETEROCYCLES, Vol. 94, No. 6, 2017, pp. 1123 - 1132. © 2017 The Japan Institute of Heterocyclic Chemistry
Received, 13th February, 2017, Accepted, 24th April, 2017, Published online, 8th May, 2017
DOI: 10.3987/COM-17-13674

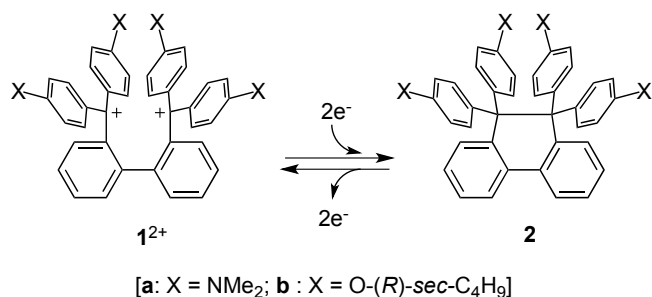
**STEREOSELECTIVE ENCAPSULATION FOR A
TRIARYLMETHYLUM *o,o*-DIMER BY NATURAL γ -CYCLODEXTRIN:
ORIGIN OF CHIRAL RECOGNITION FOR THE AXIALLY CHIRAL
DICATIONIC GUEST**

Takanori Suzuki,* José P. Cerón-Carrasco,† Hitomi Tamaoki, Yusuke Ishigaki, Ryo Katoono, Takanori Fukushima,†† and Horacio Pérez-Sánchez*,†

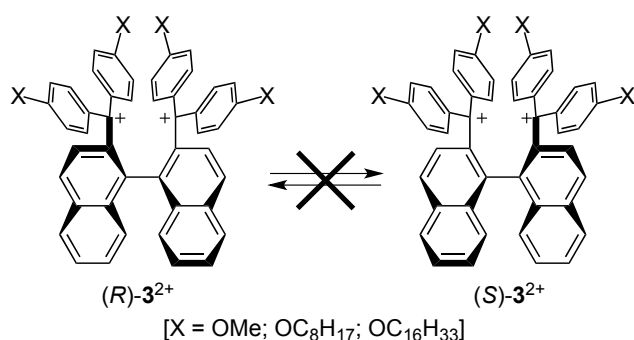
Department of Chemistry, Faculty of Science, Hokkaido University, Sapporo, Hokkaido 060-0810, Japan. †Bioinformatics and High Performance Computing Research Group (BIO-HPC), Catholic University of Murcia (UCAM), 30107 Murcia, Spain. ††Laboratory for Chemistry and Life Science, Institute of Innovative Research, Tokyo Institute of Technology, Yokohama, Kanagawa 226-8503, Japan

Abstract – Upon 1:1 complexation with γ -cyclodextrin (CyD) in water, easily interconverting rotational isomers of biphenyl-2,2'-diylbis[bis(4-dimethylaminophenyl)methylum] (*R*)/(*S*)-**1a**²⁺ were biased to prefer an *R* configuration (75 : 25 at 25 °C). Docking and quantum chemical calculations revealed two modes (on-top and bottom-side) of encapsulation of γ -CyD, which shed a light on the origin of the first chiral recognition of axially chiral dicationic dyes by using natural CyDs.

The triarylmethylum *o,o*-dimers **1**²⁺ consist of a novel class of dicationic dyes,¹ which can be converted into the corresponding 9,9,10,10-tetraaryl-9,10-dihydrophenanthrenes **2** upon two-electron reduction (Scheme 1). Thus, they are important components of novel electrochromic materials² based on the dynamic redox behavior (*dyrex* behavior)³ which is accompanied by reversible formation and cleavage of a C–C bond upon electron transfer. These dications do not prefer an extended form⁴ but a folded conformation due to π – π interaction. The face-to-face overlap of the two cationic chromophores in **1**²⁺ is evidenced by characteristic spectra in solution and also confirmed by their X-ray crystallographic analyses.⁵ For example, as shown in Figure 1, tetrakis(dimethylamino) derivative **1a**²⁺ adopts a helically

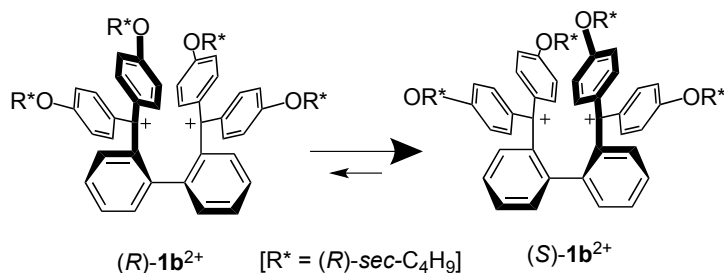


Scheme 1. "Dyrex" interconversion of 1^{2+} and 2

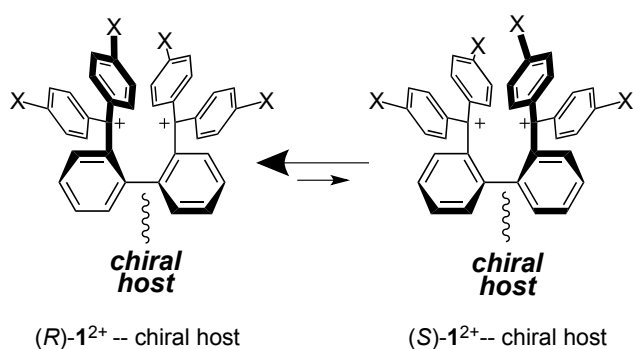


Scheme 2. Configurational stability of binaphthyl-type dications 3^{2+}

a) Intramolecular chirality transmission



b) Intermolecular chirality transmission



Scheme 3. Biasing of axial chirality in 1^{2+}

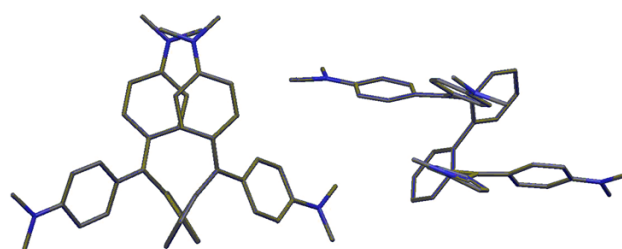
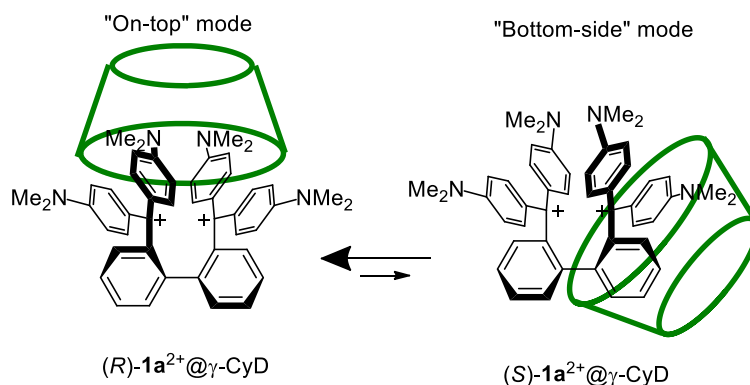


Figure 1. Two views of the X-ray structure of (*R*)- $1a^{2+}$ in its racemic ($SbCl_6$)₂ salt. The twisting angle of biphenyl and the C⁺ -- C⁺ distance are 69° and 3.66 Å, respectively.

folded conformation in the crystal⁶ with a rough dimension of W 15 x D 7 x H 10 Å. The inner two aryl groups overlap with an interplanar distance of 3.37 Å with a dihedral angle of 11.5°. A similar geometry is also expected for $1a^{2+}$ in solution since the UV-Vis spectrum exhibits well-split absorptions in the long-wavelength region [λ_{max} (ϵ)/nm in H₂O: 662 (64700), 602 (94500)] as well as in the short-wavelength Vis-region [431 (28600), 410sh (23200)]. Those pairs of absorptions result from Davydov splitting of the x-band⁷ [617 (72800)] and the less-intensive y-band⁷ [425 (15100)], respectively, of the corresponding monocation, malachite-green (MG⁺). The *N*-methyl protons of dimethylaminophenyl groups in $1a^{2+}$ appear as two singlets at 3.30 and 3.22 ppm (600 MHz, D₂O), which can be again rationalized by assuming the similar folded geometry.

The helical conformation endows 1^{2+} with strong chiroptical properties such as electronic circular dichroism (ECD).⁸ Actually, very strong bisignated Cotton effects were observed in the optically pure binaphthyl dication (*R*)- and (*S*)- 3^{2+} ,⁹ in which the rotation about the central biaryl axis is restricted by

fusing two benzene rings to $\mathbf{1}^{2+}$ (Scheme 2). However, configurational stability of the axial chirality is not the essential requirement for the dication to be ECD active. There are two ways to gain strong ECD signals for the configurationally unstable dication as shown in Scheme 3. One is the intramolecular transmission of the chiral auxiliaries to bias the preference of the



Scheme 4. Two modes of encapsulation of $\mathbf{1}^{2+}$ by γ -CyD

axial chirality, which is realized in the case of tetrakis[*(R)*-*sec*-butoxy] derivative $\mathbf{1b}^{2+}$.¹⁰ The other is the intermolecular transmission of asymmetric information to bias the sense of the axial chirality.¹¹ The latter is more challenging and still remains an important topic in the field of supramolecular chirality^{12,13} since effective chiral induction is necessary upon complexation between a chiral host molecule and an easily-racemizing guest molecule.

As the host molecules, cyclodextrins (CyDs) could be promising candidates, which exhibit excellent chiral recognition properties on helical π -systems.¹⁴ Due to the instability of cationic species in water, complexations of CyDs with carbocationic guests have not been often studied,¹⁵ however, we envisaged that polar interactions such as C-H \cdots O hydrogen bonds¹⁶ upon association may induce highly stereoselective complexation for cationic guests with CyDs. In this paper, we report that natural γ -CyD effectively forms a stable complex with the water-persistent dication $\mathbf{1a}^{2+}$,¹⁷ while inducing a preference for an *R*-configuration for the axial chirality. This is the first successful demonstration of effective transmission of the host chirality of CyD to the dicationic guest. Docking and quantum chemical calculations¹⁸ indicated two modes of encapsulation of γ -CyD toward $\mathbf{1a}^{2+}$ (Scheme 4), which confirm the preference of (*R*)- $\mathbf{1a}^{2+}$ upon complexation.

Upon gradual addition of CyDs to a dilute aqueous solution of $\mathbf{1a}^{2+}(\text{BF}_4^-)_2$ (1.0×10^{-5} M) at 25 °C, continuous changes with several isosbestic points were observed in the UV-Vis spectra for β - and γ -CyDs whereas no significant change was observed in the case of α -CyD. The spectral change continued even after 100-time addition of β -CyD whereas only 4 equivalents of γ -CyD were sufficient to achieve maximum spectral changes (Figure 2), showing that γ -CyD with a large cavity is suitable for efficient complexation with dicationic guest $\mathbf{1a}^{2+}$.

From the non-linear curve-fitting,¹⁹ a very large apparent association constant ($K_{\text{assn}} = 10^6 \text{ M}^{-1}$) was

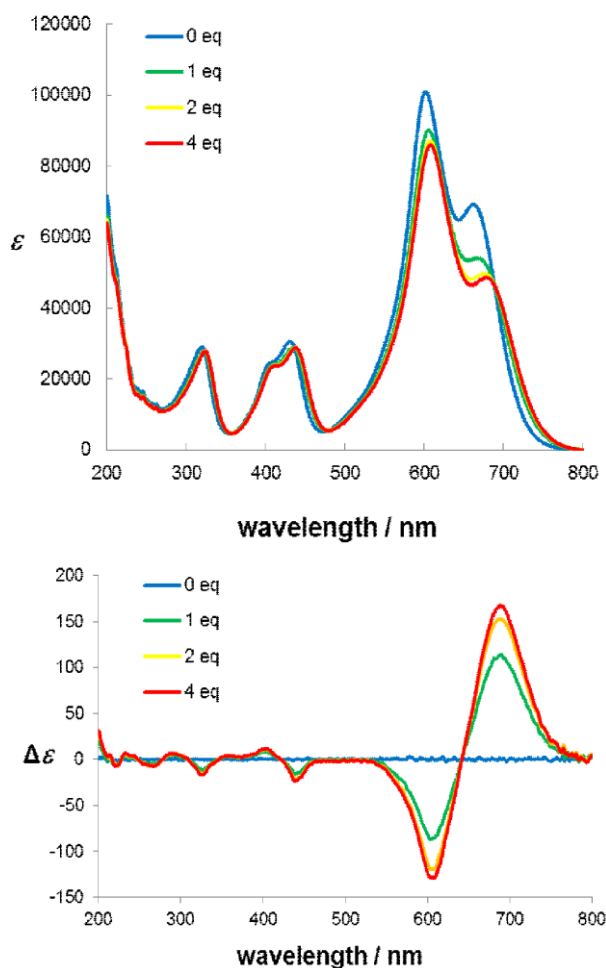


Figure 2. Changes in the (a) UV-Vis and (b) ECD spectra of $1\mathbf{a}^{2+}(\text{BF}_4)_2$ (1.0×10^{-5} M) in H_2O upon addition of γ -CyD (1 - 4 eqs) at 25 °C. Diastereomeric complexes of (*R*)- $1\mathbf{a}^{2+}@ \gamma$ -CyD and (*S*)- $1\mathbf{a}^{2+}@ \gamma$ -CyD are equilibrated over the minutes, and the ECD spectra were measured 30 min after admixing.

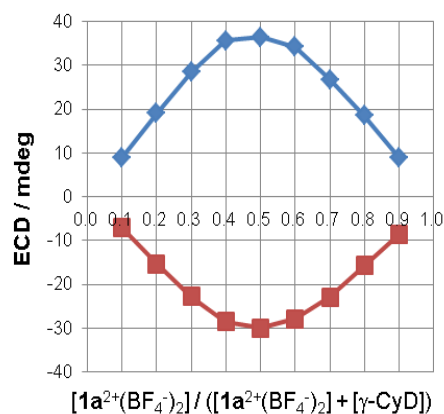


Figure 3. Job plot for the complexation of $1\mathbf{a}^{2+}(\text{BF}_4)_2$ with γ -CyD in H_2O at 25 °C using continuous changes of ECD intensity at 686 nm (blue) and 604 nm (red) ($[1\mathbf{a}^{2+}(\text{BF}_4)_2] + [\gamma\text{-CyD}] = 2.0 \times 10^{-5}$ M).

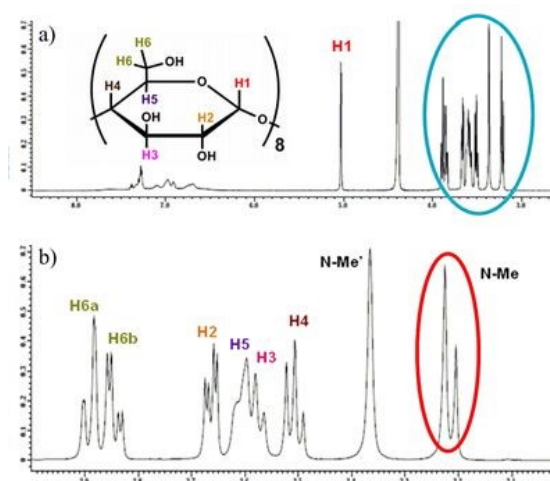


Figure 4. (a) ^1H NMR spectrum of $1\mathbf{a}^{2+}(\text{BF}_4)_2$ in the presence of γ -CyD (1.0×10^{-3} M, each) in D_2O at 65 °C. (b) Expanded spectrum of the aliphatic region.

determined for the γ -CyD complex (Figure S1). The splitted x-band of $1\mathbf{a}^{2+}$ was marginally shifted to a longer-wavelength region (λ_{max} : 680, 608 nm). Such an observation must correspond to complexation of γ -CyD and $1\mathbf{a}^{2+}$ without changing its folded conformation. Although the very large K_{assn} value is the average of those for (*R*)- and (*S*)- $1\mathbf{a}^{2+}$, the complexation must proceed diastereoselectively to prefer one-handedness of the helicity of $1\mathbf{a}^{2+}$ since the complexation-induced large amplitude²⁰ for the positive couplet at 640 nm [λ_{ext} ($\Delta\epsilon$)/nm: 686 (+155), 604 (-120)] was observed in ECD spectroscopy at 25 °C. By a Job plot of ECD, the ratio of $1\mathbf{a}^{2+}$ and γ -CyD in the complex was determined to be 1:1 (Figure 3).

Very strong ECD for $\mathbf{1a}^{2+}@_{\gamma}\text{-CyD}$ is not due to the propeller-type chiral arrangement of the triarylmethyl cation chromophores since only weak ellipticity ($\Delta\epsilon < 5$) was observed for a mixture of the monocationic MG^+BF_4^- salt and $\gamma\text{-CyD}$ in water. Thus, it is highly likely that the strong Cotton effects result from the exciton coupling of two cationic units in $\mathbf{1a}^{2+}$, which are arranged asymmetrically with a biased axial chirality of the biphenyl unit in $\mathbf{1a}^{2+}$. Based on the exciton chirality method⁸ on the less-intensive negative couplet of $\mathbf{1a}^{2+}@_{\gamma}\text{-CyD}$

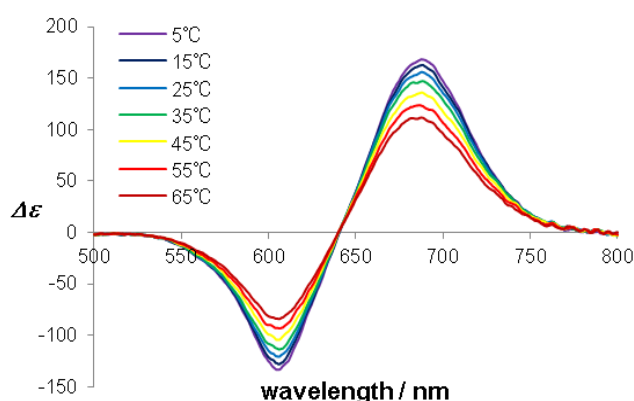


Figure 5. Temperature dependence of the ECD spectra of $\mathbf{1a}^{2+}(\text{BF}_4)_2$ (1.0×10^{-5} M) and $\gamma\text{-CyD}$ (4.0×10^{-4} M) in H_2O over 5 – 65 °C.

at 422 nm, a preference for the *R*-configuration is highly likely since the y-band shows a transition moment along the C2(biphenyl)-C(methylium) bond, and the negative couplet corresponds to counterclockwise twisting of the biphenyl axis of $\mathbf{1a}^{2+}$ in the preferred complex.

The diastereomeric excess (de) of (*R*)- $\mathbf{1a}^{2+}@_{\gamma}\text{-CyD}$ over (*S*)- $\mathbf{1a}^{2+}@_{\gamma}\text{-CyD}$ could be estimated to be 35% on the basis of ^1H NMR spectrum [$\mathbf{1a}^{2+}(\text{BF}_4)_2$ and $\gamma\text{-CyD}$ (1.0×10^{-3} M each) in D_2O at 65 °C] since the *N*-methyl protons of inner two aryl groups for the two diastereomeric complexes appear as well-separated resonances of different intensities (Figure 4). The less stable (*S*)- $\mathbf{1a}^{2+}$ complex has a resonance at 3.21 ppm, which is more shifted to the high field than that for (*R*)- $\mathbf{1a}^{2+}$ complex (3.23 ppm), showing that (*S*)- $\mathbf{1a}^{2+}@_{\gamma}\text{-CyD}$ adopts a geometry with more effective $\pi\text{-}\pi$ overlap. Although diastereoselectivity is expected to be higher at lower temperatures, temperature-dependence of de could not be fully evaluated based on NMR spectroscopy due to significant line broadening (Figure S2).

On the other hand, the complexation-induced ECD signal reversibly and steadily increases with a decrease in the temperature from 65 °C to 5 °C (Figure 5). Since the complexation equilibrium was confirmed to lie so far to $\mathbf{1a}^{2+}@_{\gamma}\text{-CyD}$ even at 65 °C under the conditions adopted in the VT-experiment ($\mathbf{1a}^{2+}$: 1.0×10^{-5} M; $\gamma\text{-CyD}$ 4.0×10^{-4} M), the ECD intensity must be proportional to the diastereomeric excess of (*R*)- $\mathbf{1a}^{2+}@_{\gamma}\text{-CyD}$ relative to (*S*)- $\mathbf{1a}^{2+}@_{\gamma}\text{-CyD}$. The high value of 50% de at 25 °C was deduced by extrapolation ($\Delta G = 0.65$ kcal mol⁻¹ at 25 °C) and demonstrates the excellent transmission of the host chirality of $\gamma\text{-CyD}$ to dicationic guest $\mathbf{1a}^{2+}$ upon complexation.

Aiming to fully capture the chemical interactions that govern the chiral recognition process, further quantum mechanical and docking simulations have been carried out, since we have already shown that molecular modeling methods are very useful for understanding the encapsulation process with CyDs.¹⁸

As illustrated in Figures 6 and 7, theoretical simulations revealed two modes of encapsulation in γ -CyD, and the stable docked structures are different for (*R*)-**1a**²⁺ (on-top mode) and (*S*)-**1a**²⁺ (bottom-side mode). Only the on-top mode of complex was obtained for (*R*)-**1a**²⁺@ γ -CyD upon docking simulations whereas only the bottom-side mode complex of (*S*)-**1a**²⁺@ γ -CyD was observed, suggesting that configuration of **1a**²⁺ completely switches preference for the encapsulation mode of γ -CyD.²¹ Although docking approach provides a valuable qualitative description of the encapsulations phenomena, more accurate quantitative analysis is required with applying higher levels of theory, e.g., quantum calculations. Consequently, the best docking poses were refined through DFT calculations by using the same M06-2X meta-hybrid functional and the larger 6-311++G(d,p) basis set to better resolve the relative energies of (*R*)-**1a**²⁺@ γ -CyD and (*S*)-**1a**²⁺@ γ -CyD. According to our calculations, the (*R*)-**1a**²⁺@ γ -CyD is 0.86 kcal mol⁻¹ more stable than its (*S*)-counterpart, which backs up the experimentally observed selectivity.

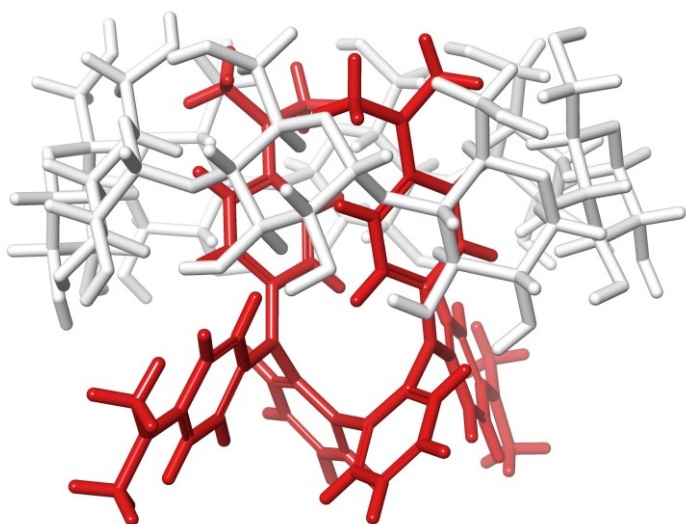


Figure 6. On-top mode encapsulation in the most stable complex of (*R*)-**1a**²⁺ with γ -CyD obtained by DFT calculation. The twisting angle of biphenyl and the C⁺ -- C⁺ distance in (*R*)-**1a**²⁺ are 74.0° and 3.91 Å, respectively.

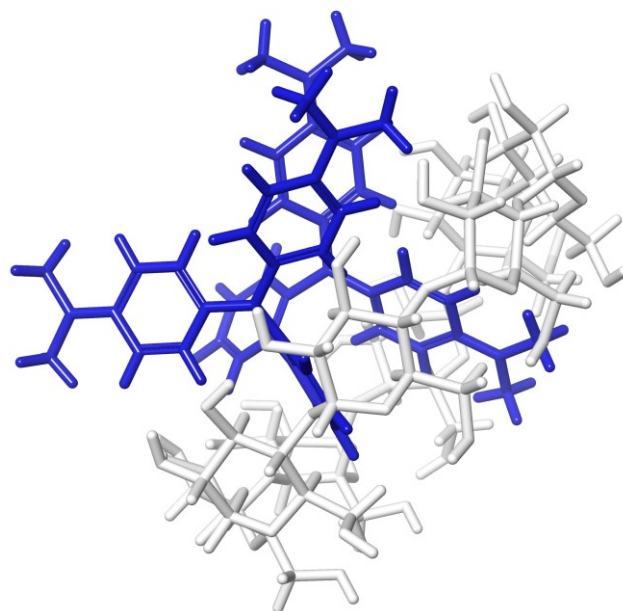


Figure 7. Bottom-side mode encapsulation in the most stable complex of (*S*)-**1a**²⁺ with γ -CyD obtained by DFT calculation. The twisting angle of biphenyl and the C⁺ -- C⁺ distance in (*S*)-**1a**²⁺ are 70.3° and 3.80 Å, respectively.

SUMMARY AND FUTURE WORKS

This paper describes the details on the first successful chiral recognition of triarylmethyl cation *o,o*-dimers **1**²⁺ by natural CyDs. Efficient complexation of tetrakis(dimethylamino) derivative (*R*)- and (*S*)-**1a**²⁺ with γ -CyD in water occurs diastereoselectively to prefer (*R*)-isomer. Although (*R*)- and (*S*)-**1a**²⁺ are easily interconvertible, the biased axial chirality could be fixed in a form with higher configurational stability. Exploring the effective chemical transformations to fix the supramolecular chirality into the molecular chirality is the next challenge of this work.¹⁷

The origin of diastereoselectivity was clarified by DFT calculations with revealing two different modes of encapsulation, and thus demonstrating the usefulness of the approach for docking and quantum chemical calculations on the CyD complexes.¹⁸ Studies on other complexes are now underway to clarify the chiral recognition properties of CyDs.

EXPERIMENTAL

Materials. CyDs are commercially available and used as received. Dicationic salt $\mathbf{1a}^{2+}(\text{BF}_4^-)_2$ was prepared as we reported previously (ref. 6)

Docking and Quantum calculations. All geometrical parameters of both (*R*)- and (*S*)-isomers of $\mathbf{1a}^{2+}$ were fully optimized at the M06-2X/6-31G(d,p) level of theory,²² as implemented in Gaussian 09.²³ Further vibrational calculations were conducted at the optimized structures to confirm that they correspond to a real minimum in the potential energy surface rather than a saddle point, which can be confirmed by the absence of any vibrational mode associated with an imaginary frequency. Atomic charges were obtained with the widely used Merz-Singh-Kollman ESP method.^{24,25}

The optimized structures of triarylmethylium *o,o*-dimers $\mathbf{1}^{2+}$ were next docked into γ -CyD. The initial γ -CyD model system was built up with the crystal structures available at Protein Data Bank²⁶ (PDB) with code 2ZYK, since it was obtained at resolutions of less than 2 Å. Molecular docking calculations were carried out using default parameters with Lead Finder.²⁷ During docking simulations γ -CyD was kept rigid, and triarylmethylium *o,o*-dimers $\mathbf{1}^{2+}$ were treated as flexible. Only the on-top mode of complex was obtained for (*R*)- $\mathbf{1a}^{2+}@ \gamma$ -CyD upon docking simulations whereas only the bottom-side mode complex of (*S*)- $\mathbf{1a}^{2+}@ \gamma$ -CyD was observed among the top ranked complexes. Eventually, the relative stability of (*R*)- $\mathbf{1a}^{2+}@ \gamma$ -CyD (on-top) and (*S*)- $\mathbf{1a}^{2+}@ \gamma$ -CyD (bottom-side) is predicted by directly comparing the total electronic energy of best poses at the M06-2X/6-311++G(d,p) level of theory in kcal mol⁻¹.

ACKNOWLEDGEMENTS

We thank Grant-in-Aid for Scientific Research on Innovative Areas: "Middle molecular strategy" (No. 2707) from MEXT and Grant-in-Aid from JSPS (Nos. JP15H03790, JP16K13968, JP15K17818, JP16H06591) Japan. This work was also supported by the Research Program of "Five-star Alliance" in "NJRC Mater. & Dev" (MEXT). This work was partially supported by the Fundación Séneca–Agencia de Ciencia y Tecnología de la Región de Murcia under Projects 18946/JLI/13 and 19419/PI/14-1. Powered@NLHPC: This research was partially supported by the supercomputing infrastructure of the NLHPC (ECM-02). The authors also thankfully acknowledge the computer resources and the technical support provided by the Plataforma Andaluza de Bioinformática of the University of Málaga. This work

was partially supported by the computing facilities of Extremadura Research Centre for Advanced Technologies (CETA–CIEMAT), funded by the European Regional Development Fund (ERDF). CETA–CIEMAT belongs to CIEMAT and the Government of Spain.

REFERENCES AND NOTES

1. T. Suzuki, T. Takeda, E. Ohta, K. Wada, R. Katoono, H. Kawai, and K. Fujiwara, *Chem. Rec.*, **2015**, [15](#), 280; T. Suzuki, E. Ohta, H. Kawai, K. Fujiwara, and T. Fukushima, *Synlett*, **2007**, 851.
2. P. M. S. Monk, R. J. Mortimer, and D. R. Rosseinsky, *'Electrochromism and Electrochromic Devices'*, Cambridge Univ. Press, Cambridge, **2007**.
3. T. Suzuki, H. Tamaoki, J. Nishida, H. Higuchi, T. Iwai, Y. Ishigaki, K. Hanada, R. Katoono, H. Kawai, K. Fujiwara, and T. Fukushima, 'Organic Redox Systems: Synthesis, Properties and Applications, Chapter 2 Redox-mediated reversible σ -bond formation/cleavage', Wiley, 2015, pp. 13-38; T. Suzuki, H. Higuchi, T. Tsuji, J. Nishida, Y. Yamashita, and T. Miyashi, 'Chemistry of Nanomolecular Systems. Chapter 1: Dynamic Redox Systems', Springer, Heidelberg, 2003, pp. 3-24.
4. The extended form with an *anti*-conformation was observed in the 2,2'-bipyridyl-6,6'-diyl dication, in which the nitrogen atom coordinates to the cationic center of diarylmethylmethyl units: T. Suzuki, R. Tamaki, E. Ohta, T. Takeda, H. Kawai, K. Fujiwara, and M. Kato, *Tetrahedron Lett.*, **2007**, [48](#), 3823.
5. Y. Sakano, R. Katoono, K. Fujiwara, and T. Suzuki, *Chem. Commun.*, **2015**, [51](#), 14303; T. Suzuki, Y. Kuroda, K. Wada, Y. Sakano, R. Katoono, K. Fujiwara, F. Kakiuchi, and T. Fukushima, *Chem. Lett.*, **2014**, [43](#), 887; T. Suzuki, K. Ohta, T. Nehira, H. Higuchi, E. Ohta, H. Kawai, and K. Fujiwara, *Tetrahedron Lett.*, **2008**, [49](#), 772.
6. T. Suzuki, J. Nishida, and T. Tsuji, *Angew. Chem., Int. Ed. Engl.*, **1997**, [36](#), 1329.
7. C. W. Looney and W. T. Simpson, *J. Am. Chem. Soc.*, **1954**, [76](#), 6293.
8. N. Berova, K. Nakanishi, and R. W. Woody, 'Circular Dichroism: Principles and Applications', 2nd edn., Wiley-VCH, New York, 2000.
9. T. Suzuki, Y. Ishigaki, T. Iwai, H. Kawai, K. Fujiwara, H. Ikeda, Y. Kano, and K. Mizuno, *Chem. Eur. J.*, **2009**, [15](#), 9434; J. Nishida, T. Suzuki, M. Ohkita, and T. Tsuji, *Angew. Chem. Int. Ed.*, **2001**, [40](#), 3251.
10. T. Suzuki, T. Iwai, E. Ohta, H. Kawai, and K. Fujiwara, *Tetrahedron Lett.*, **2007**, [48](#), 3599.
11. J. Setsune, A. Tsukajima, N. Okazaki, J. M. Lintuluoto, and M. Lintuluoto, *Angew. Chem. Int. Ed.*, **2009**, [48](#), 771; R. Randazzo, A. Mammana, A. D'Urso, R. Lauceri, and R. Purrello, *Angew. Chem. Int. Ed.*, **2008**, [47](#), 9879; **2009**, [48](#), 1351; M. Ishikawa, K. Maeda, Y. Mitsutsuji, and E. Yashima, *J. Am. Chem. Soc.*, **2004**, [126](#), 732; T. Ishi-i, M. Crego-Calama, P. Timmerman, D. R. Reinhoudt, and S.

- Shinkai, *J. Am. Chem. Soc.*, 2002, **124**, 14631; E. Yashima, K. Maeda, and Y. Okamoto, *Nature*, 1999, **399**, 449; Y. Mizuno, T. Aida, and K. Yamaguchi, *J. Am. Chem. Soc.*, 2000, **122**, 5278.
12. R. Katoono, 'Synergy in Supramolecular Chemistry, Chapter 14: Design of chirality-sensing systems based on supramolecular transmission of chirality', CRC press, 2015, pp. 247-260; G. A. Hembury, V. V. Borovkov, and Y. Inoue, *Chem. Rev.*, 2008, **108**, 1; A. R. A. Palmans and E. W. Meijer, *Angew. Chem. Int. Ed.*, 2007, **46**, 8948; R. Purrello, *Nat. Mater.*, 2003, **2**, 216.
13. R. D. Rasberry, X. Wu, B. N. Bullock, M. D. Smith, and K. D. Shimizu, *Org. Lett.*, 2009, **11**, 2599; T. Miyabe, Y. Hase, H. Iida, K. Maeda, and E. Yashima, *Chirality*, 2009, **21**, 44; N. Ousaka, Y. Inai, and R. Kuroda, *J. Am. Chem. Soc.*, 2008, **130**, 12266.
14. K. Kano, K. Imaeda, K. Ota, and R. Doi, *Bull. Chem. Soc. Jpn.*, 2003, **76**, 1035; K. Kano, H. Kamo, S. Negi, T. Kitae, R. Takaoka, M. Yamaguchi, H. Okubo, and M. Hirama, *J. Chem. Soc., Perkin Trans. 2*, 1999, 15; S. Y. Yang, M. M. Green, G. Schultz, S. K. Jha, and A. H. E. Müller, *J. Am. Chem. Soc.*, 1997, **119**, 12404.
15. T. C. Barros, S. H. Toma, H. E. Toma, E. L. Bastos, and M. S. Baptista, *J. Phys. Org. Chem.*, 2010, **23**, 893; L. García-Río and A. Godoy, and J. R. Leis, *Chem. Phys. Lett.*, 2005, **401**, 302; R. L. Schiller, J. H. Coates, and S. F. Lincoln, *J. Chem. Soc., Faraday 1*, 1984, **80**, 1257.
16. J. Bernstein, *Cryst. Growth Des.*, 2013, **13**, 961; C. H. Schwalbe, *Crystallogr. Rev.*, 2012, **18**, 191; T. Steiner, G. Koellner, K. Gessler, and W. Saenger, *J. Chem. Soc., Chem. Commun.*, 1995, 551; G. R. Desiraju, *Acc. Chem. Res.*, 1991, **24**, 290; R. Taylor and O. Kennard, *Acc. Chem. Res.*, 1984, **17**, 320.
17. A part of this paper was published as a preliminary communication: T. Suzuki, H. Tamaoki, K. Wada, R. Katoono, T. Nehira, H. Kawai, and K. Fujiwara, *Chem. Commun.*, 2012, **48**, 2812.
18. J. P. Cerón-Carrasco, H. den-Haan, J. Peña-García, J. Contreras-García, and H. Pérez-Sánchez, *Comp. Theor. Chem.*, 2016, **1077**, 65; S. López-Miranda, A. Serrano-Martínez, P. Hernández-Sánchez, L. Guardiola, H. Pérez-Sánchez, I. Fortea, J. A. Gabaldón, and E. Núñez-Delicado, *Food Chem.*, 2016, **203**, 379; I. Terekhova, R. Kumeev, G. Alper, S. Chakraborty, H. Pérez-Sánchez, and E. Núñez-Delicado, *RSC Adv.*, 2016, **6**, 49567; G. Budryn, B. Palecz, D. Rachwal-Rosiak, J. Oracz, D. Zaczynska, S. Belica, I. Navarro-González, J. Vegara-Meseguer, and H. Pérez-Sánchez, *Food Chem.*, 2015, **168**, 276; J. M. López-Nicolas, M. Escorial-Camps, H. Pérez-Sánchez, and F. García-Carmona, *J. Agric. Food Chem.*, 2013, **61**, 11347.
19. W. Al-Soufi, P. R. Cabrer, A. Jover, R. M. Budal, and J. V. Tato, *Steroids*, 2003, **68**, 43.
20. G. Gottarelli, S. Lena, S. Masiero, S. Pieraccini, and G. P. Spada, *Chirality*, 2008, **20**, 471; D. Krois and U. H. Brinker, 'Cyclodextrins and Their Complexes', pp. 289-298, Wiley-VCH, Weinheim, 2006.
21. Preliminary results on the calculation of $1\mathbf{a}^{2+}$ with β -CyD show that only the bottom-side mode of encapsulation was obtained irrespective to the configuration of *R* or *S*.

22. Y. Zhao and D. G. Truhlar, [Acc. Chem. Res.](#), 2008, **41**, 157.
23. *Gaussian 09, Revision E.01*, M. J. Frisch, G. W. Trucks, H. B. Schlegel, G. E. Scuseria, M. A. Robb, J. R. Cheeseman, G. Scalmani, V. Barone, B. Mennucci, G. A. Petersson, H. Nakatsuji, M. Caricato, X. Li, H. P. Hratchian, A. F. Izmaylov, J. Bloino, G. Zheng, J. L. Sonnenberg, M. Hada, M. Ehara, K. Toyota, R. Fukuda, J. Hasegawa, M. Ishida, T. Nakajima, Y. Honda, O. Kitao, H. Nakai, T. Vreven, J. A. Montgomery, Jr., J. E. Peralta, F. Ogliaro, M. Bearpark, J. J. Heyd, E. Brothers, K. N. Kudin, V. N. Staroverov, R. Kobayashi, J. Normand, K. Raghavachari, A. Rendell, J. C. Burant, S. S. Iyengar, J. Tomasi, M. Cossi, N. Rega, J. M. Millam, M. Klene, J. E. Knox, J. B. Cross, V. Bakken, C. Adamo, J. Jaramillo, R. Gomperts, R. E. Stratmann, O. Yazyev, A. J. Austin, R. Cammi, C. Pomelli, J. W. Ochterski, R. L. Martin, K. Morokuma, V. G. Zakrzewski, G. A. Voth, P. Salvador, J. J. Dannenberg, S. Dapprich, A. D. Daniels, Ö. Farkas, J. B. Foresman, J. V. Ortiz, J. Cioslowski, and D. J. Fox, *Gaussian, Inc., Wallingford CT*, 2009.
24. U. C. Singh and P. A. Kollman, [J. Comput. Chem.](#), 1984, **5**, 129.
25. B. H. Besler, K. M. Merz Jr., and P. A. Kollman, [J. Comput. Chem.](#), 1990, **11**, 431.
26. J. L. Sussman, L. Dawei, J. Jiansheng, N. O. Manning, J. Prilusky, O. Ritter, and E. E. Abola, [Acta Crystallogr. Sect. D- Biol. Crystallogr.](#), 1998, **54** 1078.
27. O. Stroganov, [J. Chem. Inf. Model.](#), 2008, **48**, 2371.